Metal-Fluorocarbon-Pyrolants IV: Thermochemical and Combustion Behaviour of Magnesium/Teflon/Viton (MTV)

Ernst-Christian Koch*

Diehl Munitionssysteme GmbH & CO. KG, Karl-Diehl-Str. 1, D-66620 Nonnweiler (Germany)

Summary

The thermochemical and combustion behaviour of pyrotechnic payloads based on magnesium, Teflon® and Viton®, so-called MTV is discussed. Thermochemical and FTIR-spectroscopic analysis of magnesium/Teflon® combustion residues indicates the intermediate formation of a Grignard-type C–Mg–F compound in the condensed phase as part of a preignition reaction (PIR). The PIR is mainly responsible for the observed burning rate which rises exponentially with rising magnesium weight fractions from $\xi(Mg) \sim 0.2$ to $\xi(Mg) \sim 0.70$ and declines at $\xi(Mg) > \sim 0.70$. A tentative mechanism for the combustion process is presented. For part III see Ref. 1.

1 Introduction

Pyrolants based on **M**agnesium (Mg), **T**eflon®** (polytetrafluoroethylene) (acr. PTFE) ($(-C_2F_4-)_n$) and **V**iton® (hexafluoropropene-vinylidenefluoride-copolymer) ($(-C_5H_3F_8-)_n$) so-called **MTV** are widely applied in either technical and military pyrotechnics[1]. In the present paper the thermochemical properties and the combustion characteristics of this material are discussed.

2 Thermochemical Properties

The main parameters characterizing pyrotechnic payloads are the adiabatic flame temperature T_f (K), the linear burning rate r ($mm \cdot s^{-1}$), the mass consumption rate $\dot{m}$ ($g \cdot s^{-1} \cdot cm^{-2}$), the pressure exponent n (1) related to the burning rate law $r = a \cdot p^n$ and the specific heat of combustion Q ($kJ \cdot g^{-1}$). These parameters will be discussed in the following section.

2.1 Properties of the Components

The constituents of MTV are magnesium, polytetrafluoroethylene (PTFE) and hexafluoropropene-vinylidenefluoride-copolymer (Viton®). Their thermochemical properties are presented in Table 1.

2.2 Flame Temperature

2.2.1 Adiabatic Flame Temperature

The adiabatic flame temperature T_f of a system is an important parameter to characterize a pyrotechnic composition in terms of "how hot is the flame". In general, experimental measurement or theoretical determination of the flame temperature of a burning pyrotechnic composition is always associated with some degree of uncertainty. Thus values obtained by either practical or theoretical methods should be regarded as more or less rough figures helping to compare the system under investigation to other known systems.

A common numerical computer code to calculate both the adiabatic flame temperature at a chosen pressure and molar fractions of combustion products is the NASA-CEA program[2]. Figure 1 shows the adiabatic flame temperature and weight fractions of major combustion products calculated using the CEA code in the range $\xi(Mg)$ 0.05 – 0.63 at 0.1 MPa.

The stoichiometric formulations investigated are given by the broken line through the diagram in Figure 1 at

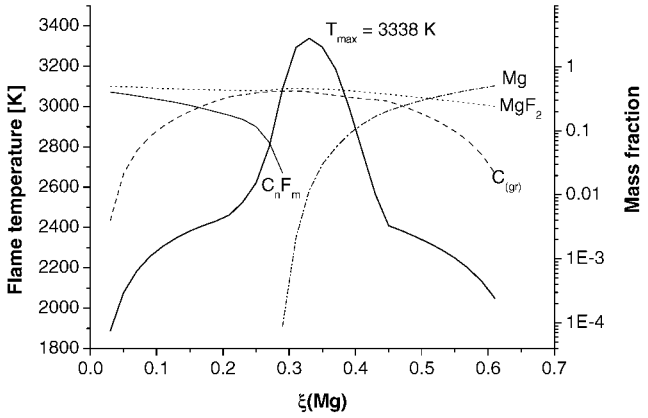

Figure 1. Flame temperatures and weight fractions of major combustion products at 0.1 MPa.

* Corresponding author; e-mail: ernst.christian.koch@diehl-mun.de

** Teflon (polytetrafluoroethylene) and Viton (hexafluoropropene-vinylidenefluoride-copolymer) are trademarks of DuPont.

 0721-3113/02/2706-0340 $ 17.50+.50/0

Table 1. Thermochemical properties of MTV constituents.

Parameter	Unit	Mg	MgF_2	$(-C_2F_4-)_n$	$(-CH_2-CF_2-)-(CF(CF_3)CF_2-)_n$
CAS-Nr.		7439-95-4	7783-40-6	9002-84-0	9011-17-0
m_r	g mol^{-1}	24.305	62.302	100.02	374.145
T_{mp}	°C	648.8	1263	324	decomposition
T_{bp}	°C	1090	2239	decomposition	n.a.
$\rho_{20°C}$	g cm^{-3}	1.738	3.148	2.31	1.85
ΔH_f^{298}	kJ mol^{-1}	0	– 1124	– 809.60	– 2784.03
ΔH_{melt}^{298}	kJ mol^{-1}	– 9.04	– 58.2	– 3.6	n.a.
ΔH_{vap}^{298}	kJ mol^{-1}	– 127.6	– 247.1	n.a.	n.a.
ΔH_{dep}^{298}	kJ mol^{-1}	n.a.	n.a.	– 172	– 128
c_p^{298}	J g^{-1} K^{-1}	1.023	0.988	1.020	1.30
λ	W m^{-1} K^{-1}	156.000	~10	0.244	0.130

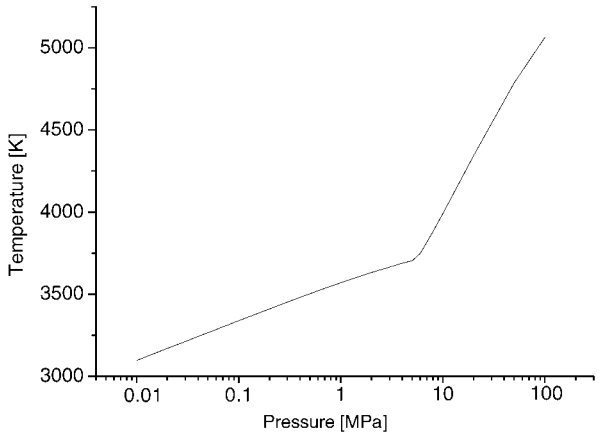

Figure 2. Variation of the adiabatic flame temperature at $\xi(Mg) = 0.32$ versus pressure with $p = 0.01 - 10$ MPa.

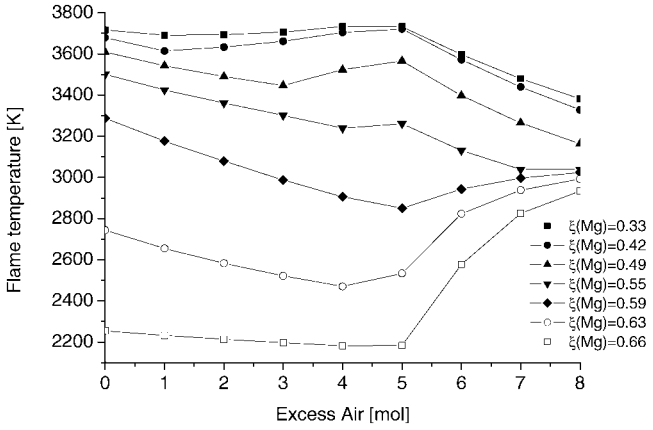

Figure 3. Variation of the adiabatic flame temperature at various $\xi(Mg)$ as function of excess air added on a per mole magnesium basis.

ξ (Viton®) = 0.05 of Ref. 1. The maximum attainable flame temperature under adiabatic conditions is 3338 K. The variation of the adiabatic flame temperature versus pressure is given in Figure 2. The steeper increase in T_f at $p > 8$ MPa is a result of the increasing number of combustion species with low c_p.

2.2.2 Real Flame Temperature

It is quite complicated to aim at the calculation of realistic flame temperatures under combustion of a pyrolant in air. Whereas addition of surplus air may lead to a depression in flame temperature at the stoichiometric ratio, the flame temperature of fuel rich compositions is increased by after burn reactions in the plume as has also been observed with $Mg/NaNO_3$ pyrolants[3]. A common approach is to assume the air to be an additional composition ingredient as has been done by DeYong and Smit[4]. Nevertheless, Christo[5] has employed a more realistic approach in reacting the primary combustion products with the air at the given flame temperature. Figure 3 thus shows the variation of flame temperature of the Mg/PTFE pyrolant with rising air entrainment in the combustion zone at different stoichiometries.

Considering the radiation behaviour of MTV, which will be addressed in an upcoming paper, it becomes evident that afterburn reactions, that are reactions of the primary (anaerobic) combustion products with air, determines largely the radiant behaviour of MTV flares.

2.3 DSC, DTA, DTG Investigations

Important tools characterizing the combustion mechanism of pyrotechnic systems are thermoanalytical methods such as DSC, DTA and DTG.

2.3.1 Decomposition of Polytetrafluoroethylene

The combustion mechanism of MTV requires at first the knowledge of the thermal decomposition reaction of PTFE.

DTA measurement of PTFE under air reveals melting at ~327 °C[6]. Between ambient temperature and the melting point the volume of PTFE expands to 120% of the original volume[7]. At 460 °C an exothermal decomposition reaction accompanied by weight loss starts and is completed at ~610 °C where all of the starting material has been consumed (100% weight loss).

The constituents of the thermal decomposition reaction in air (Eqs. 1a and 1b) are mainly carbonyl difluoride (COF_2), tetrafluoroethylene (C_2F_4) and difluorocarbene ($:CF_2$)[8].

$$(-C_2F_4-)_n \xrightarrow[air]{\Delta} nCOF_2 + \frac{n}{2}(C_2F_4) \quad (1a)$$

$$(C_2F_4) \xrightarrow{\Delta} 2{:}\,CF_2 \quad (1b)$$

Δ = heat

In presence of humidity also hydrogen-containing products such as fluoroform (CHF_3) and hydrogen fluoride are formed (Eqs. 2a and 2b).

$$COF_2 + H_2O \rightarrow CO_2 + HF \quad (2a)$$

$$:CF_2 + HF \rightarrow CHF_3 \quad (2b)$$

In addition, the thermal decomposition of PTFE has been studied in vacuum. Under this condition, the decomposition is an endothermic process yielding a mixture of the monomer and acyclic as well as cyclic fluorocarbons (Eq. 3).

$$(-C_2F_4-)_n \xrightarrow[vacuo]{\Delta} nC_2F_4 + \frac{n}{10}(C_3F_8 + cyclo - C_4F_8) \quad (3)$$

Under argon gas, the decomposition starts at 512 °C and in nitrogen at 486 °C[9]. Similarly decomposition under inert atmosphere is an endothermic process yielding a similar product distribution as under vacuum.

The distribution of PTFE decomposition products at typical pyrotechnic combustion temperatures (1000–5000 K) has been calculated on the basis of local thermodynamic equilibrium (LTE) by Speckhofer et al.[10]. They revealed the main constituents to be difluorocarbene, tetrafluoromethane (CF_4), solid carbon ($C_{(s)}$) and atomic fluorine ($F_{(g)}$). Especially, difluorocarbene has been identified to be the major decomposition product of the superior oxidizer poly(carbon monofluoride) ($(-CF-)_n$)[11,12].

It has been found, that the release of gaseous products upon thermal treatment of PTFE may be suppressed by addition of nonvolatile basic compounds such as calcium hydroxide ($Ca(OH)_2$) and sodium hydroxide (NaOH)[13].

2.3.2 Decomposition of the Magnesium/Polytetrafluoroethylene Mixture (MT)

Since Viton® is included in MTV compositions only for manufacturing purposes, it serves for coating of magnesium and allows molding ($\leq 5\%$) and extrusion of MTV ($\leq 16\%$), dependent on the weight fraction. It will not be considered here. Therefore, the simplified Magnesium/Teflon® system (MT) will be treated.

Very early DTA/TG measurements on MT compositions have been reported by Krien[14]. With $\xi(Mg) = 0.59$ the investigated system can be considered as fuel rich. The DTA plot shows at first the melting endothermal peak at 325 °C followed by a sharp exothermal for the decomposition of PTFE at 479 °C. A second endothermal peak at 645 °C is assigned to the melting of magnesium that subsequently starts to be oxidized in the air at 700 °C.

Griffiths et al. performed a series of DTA measurements on fuel rich Mg/PTFE mixtures[9]. They found the endothermic decomposition of PTFE to become exothermic when adding magnesium and subsequently rising related to $\xi(Mg)$. This observation is not surprising since the polymerisation of tetrafluoroethylene, according to Eq. 4, is an exothermic process.

$$nC_2F_4 \xrightarrow{polymerisation} (-C_2F_4-)_n + n \cdot 172\ \text{kJ} \quad (4)$$

Thus the thermal decomposition under inert atmosphere of PTFE is the reverse reaction and requires an energy input equal to the heat amount released during polymerisation. By the presence of magnesium the heat of formation of magnesium fluoride compensates the endothermic depolymerization of PTFE.

In addition, the DTA plots show a complex series of reactions in the condensed state. Nevertheless, the melting endothermal peak for magnesium in either stoichiometric or fuel rich MT compositions indicates an incomplete reaction of magnesium with either PTFE or volatile fluorocarbon compounds.

A series of DTA measurements on Mg/PTFE compositions also were conducted by Cudzilo[15,16].

2.3.2.1 Experiments on the Decomposition of Magnesium/Polytetrafluoroethylene mixture (MT)

DSC analysis was performed with a consolidated stoichiometric MT composition, ($\xi(Mg) = 0.32$) in an aluminium crucible with perforated cap and constant argon flow ($52\ ml \cdot min^{-1}$) at a heating rate of $5\ K \cdot min^{-1}$. After melting of PTFE at 332 °C, the onset of a first exothermic reaction is at 394 °C. The tentative maximum of this reaction is a shoulder at 441 °C. The onset of a second exothermic reaction, which superimposes the first reaction, is at 447 °C. This reaction displays a distinct maximum peak at 509 °C. At 540 °C a shoulder indicates a third exothermic reaction, which is completed at 553 °C. A fourth exothermic reaction has its peak value at 575 °C that is finished at 590 °C. The enthalpy of reaction of the first three reactions is $\sim 300\ J \cdot g^{-1}$. The fourth reaction provides another $140\ J \cdot g^{-1}$.

To get insight in the reactions occurring in the DSC experiment of the stoichiometric MT mixture up to 600 °C the residue has been investigated by means of FTIR-spectroscopy.

Figure 4 displays the FTIR-spectra in a KBr matrix of the residue of the DSC experiment as well as the residue heated under Argon to 700 °C.

A broad intense peak at $3429\ cm^{-1}$ is due to water. The signal at $1634\ cm^{-1}$ can be assigned to conjugated C=C units. The intense peak at $1413\ cm^{-1}$ with a shoulder at higher wave number is tentatively assigned to a fluorinated olefin

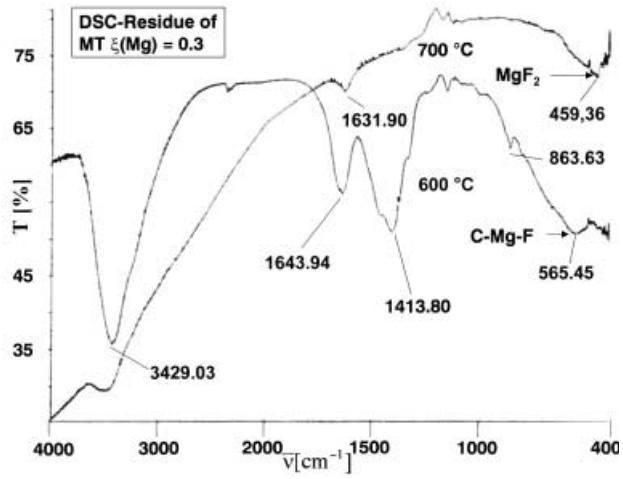

Figure 4. FTIR-absorption spectra.

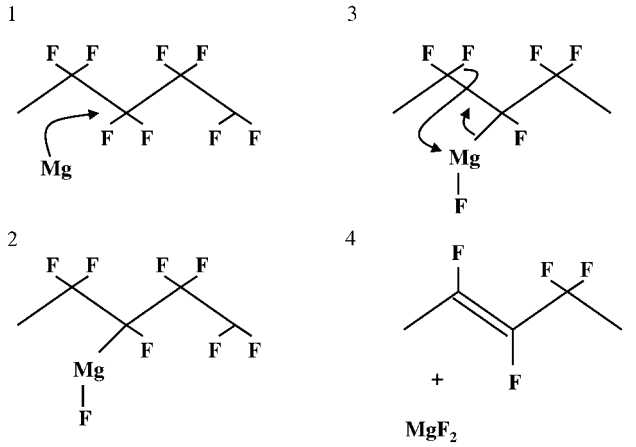

Scheme 1. Proposed reductive elimination of fluorine from PTFE applying magnesium under DSC experiment conditions.

unit C=C–F[17]. Due to the absence of a peak at ~456 cm^{-1} that would identify MgF_2, the signal at 565 cm^{-1} is tentatively assigned to an Mg-C-F- unit[18].

The spectrum of the DSC residue thus shows complete conversion of PTFE, which would yield peaks at 1220, 1150, 640 and 500 cm^{-1}. The peaks found for the olefinic units at 1634 and 1413 cm^{-1} indicate a stepwise mechanism of the reaction between Mg and PTFE at chosen DSC conditions.

Dykstra and Jasien had postulated the possible existence of the hitherto unknown solid Grignard-type compounds having C–Mg–F units as early as 1983[19,20]. They calculated the exothermicity of the insertion step of Mg in simple methyl fluoride (CH_3F), Eq. (5)

$$Mg + CH_3F \rightarrow CH_3MgF + 242\ \text{kJ} \tag{5}$$

to provide as much as 242 $kJ \cdot mol^{-1}$.

Liu and Davies recently performed ab-initio calculations on the reaction between fluoroethylene and magnesium as well as fluoromethane and magnesium[21,22]. They postulated a Grignard-type reaction between PTFE and Mg to be one possible starting reaction upon combustion of MTV. These authors calculated the heat of reaction between magnesium and fluoroethylene, Eq. (6) with several computational methods to equal values between 170–260 $kJ \cdot mol^{-1}$.

$$Mg + C_2H_3F \rightarrow C_2H_3MgF + \left(170 - 260\ \text{kJ} \cdot \text{mol}^{-1}\right) \tag{6}$$

In view of this it is not unlikely to assume a reductive elimination of fluorine from the carbon backbone of PTFE yielding partially olefinic units (Scheme 1).

It is obvious that this type of reaction may not account for the whole combustion mechanism, but it is likely to assume this reaction sequence as part of the **p**rei**g**nition **r**eaction (PIR) in the condensed phase beneath the burning surface.

To prove for the intermediate formation of a fluoro Grignard-type compound a part of the DSC sample residue was heated under Argon atmosphere to 700 °C for at least 10 min. The FTIR analysis shows a signal at 459 cm^{-1} indicating the formation of MgF_2 and still shows presence of olefinic units due to broad peaks between 1650–1400 cm^{-1}.

This confirms the proposed reaction sequence which in case of the DSC experiment would stop at 600 °C at the stage of the fluoro Grignard-type intermediate (Eq. 6) that had been postulated[21].

3 Combustion Mechanism

The combustion of heterogeneous energetics consists of the condensed phase combustion not involving the gas phase and the gas phase combustion. Neither of these cases may completely account for a real system but a combination of both may describe a real system such as MTV.

As discussed above, MTV displays a preignition reaction associated with the Grignard reaction, Eq. (7), that could provide enough heat in the condensed phase and thus promote liquefaction and vaporization of magnesium, Eq. (8), as well as decomposition of PTFE, Eq. (9) and thus enable gas phase combustion of magnesium and the monomer, Eq. (10). Later we will try to determine the contribution of both these partial reactions to the burning rate (c.f. Section 3.1.4)

$$Mg_{(s)} + (-C_2F_4-)_{n,liquid} \xrightarrow{\Delta} MgF_{2(s)} + (-CF=CF-)_{n,liquid} + Q \tag{7}$$

$$Mg_{(s)} + Q \rightarrow Mg_{(l,g)} \tag{8}$$

$$(-C_2F_4-)_{n,liquid} + Q \rightarrow nC_2F_{4(g)} \tag{9}$$

$$2Mg_{(l,g)} + C_2F_{4(g)} \rightarrow 2MgF_{2(l,s)} + 2C_{(s)} + Q \tag{10}$$

Two important issues considering the combustion process of MTV are the "chemical environment" of the fluorine as well as the distinction between gas phase and multi phase combustion mechanism.

Addressing the "chemical environment" of fluorine we may assume that the PTFE polymer is decomposed to yield gaseous tetrafluoroethylene (C_2F_4). This at the high combustion temperatures of MTV (~3000 K) will certainly decompose to give more stable species as has been calculated[10]. Thus the product distribution at 3000 K is $\xi(:CF_2) = 0.30$, $\xi(C) = 0.29$, $\xi(CF_4) = 0.29$, $\xi(F) = 0.05$, $\xi(\cdot CF_3) = 0.05$, $\xi(:CF) = 0.02$. Hence the main fluorine sources are difluorocarbene ($:CF_2$) and tetrafluoromethane (CF_4). These compounds will be considered to interact with the magnesium "dispersed" in the gas phase. A kinetics sensitivity analysis on the combustion of MTV by Christo[5] confirms the assumption, that difluorocarbene is the major oxidizing specie of the combustion of MTV.

With respect to afterburn reactions, the reaction of tetrafluoroethylene with atmospheric oxygen to yield carbonyl fluoride, as well as the oxidation of solid carbon to give carbon oxides and finally oxidation of surplus magnesium by either oxygen or carbon oxides has to be considered.

The following reactions with respective equilibrium flame temperatures[2] have to be considered for the combustion process of MT in air. They can be separated in primary, anaerobic reactions:

$$Mg_{(l,g)} + CF_{4(g)} \rightarrow MgF_{2(l)} + :CF_{2(s)} \quad T_{eq} = 2428\ \text{K} \tag{11}$$

$$Mg_{(l,g)} + :CF_{2(g)} \rightarrow MgF_{2(g)} + C_{(s)} \quad T_{eq} = 3627\ \text{K} \tag{12}$$

and secondary, aerobic reactions

$$C_2F_4 + O_2 \rightarrow 2COF_2 \quad T_{eq} = 2365\ \text{K} \tag{13}$$

$$xC + nO_2 \rightarrow yCO + zCO_2\ T_{eq} \text{ dependent on } n \text{ and } x \tag{14}$$

$$Mg_{(l,g)} + COF_{2(g)} \rightarrow MgF_{2(l,g)} + CO_{(g)} \quad T_{eq} = 2471\ \text{K} \tag{15}$$

$$Mg_{(l,g)} + CO_{(g)} \rightarrow MgO_{(s)} + C_{(s)} \quad T_{eq} = 2050\ \text{K} \tag{16}$$

$$Mg_{(l,g)} + {}^1\!/_2 O_{2(g)} \rightarrow MgO_{(s)} \quad T_{eq} = 3388\ \text{K} \tag{17}$$

Christo has reported kinetic data on some of these elementary reactions assumed to occur as well as some sensitivity analysis on certain key reactions[5]. Thus the most important reaction is assumed to be Eq. (12).

According to Glassman's criteria for metal combustion[23] the combustion of metals in oxygen occurs in the vapour phase if the metal boiling point is lower than the boiling point of the oxide. If we assume this hypothesis valid for the interaction of magnesium and fluorine and chemically bound fluorine, then from Table 1 we can assume that gas phase fluorination of magnesium occurs.

IR emission spectroscopy of burning MTV mainly shows a grey body type intensity distribution[24] (Figure 5) which is superimposed on molecular bands from both H_2O, CO and CO_2 due to afterburn reactions in the plume. Although the IR range gives no information on the phases involved in the primary combustion process strong selective emissions in the UV[25] indicate gas phase combustion of Mg due to emission from gaseous $MgF_{(g)}$ at 340–370 nm. This confirms the assumed, at least partial, gas phase combustion of magnesium in fluorine environment. In addition to that, equilibrium chemical composition calculation for various MT stoichiometries (see Figure 1) also points out for substantial amounts of gaseous MgF_2 and MgF[2].

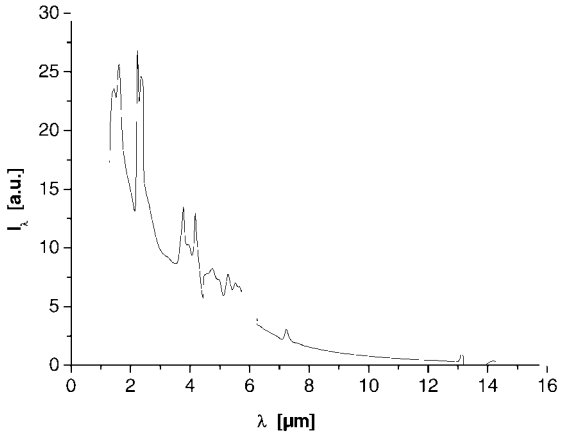

Figure 5. FTIR-emission spectrum of MTV at $\xi(Mg) = 0.32$.

The schemes 2a and 2b show the proposed reaction path in both the condensed and the gas phase.

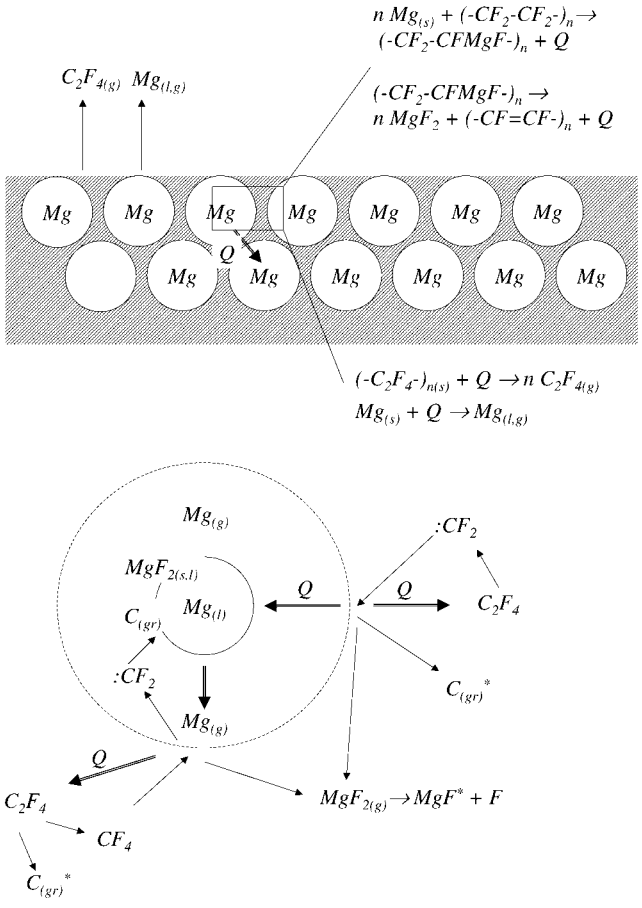

Scheme 2. Proposed reaction path of MT combustion in both condensed phase **a)** and gas phase **b).**

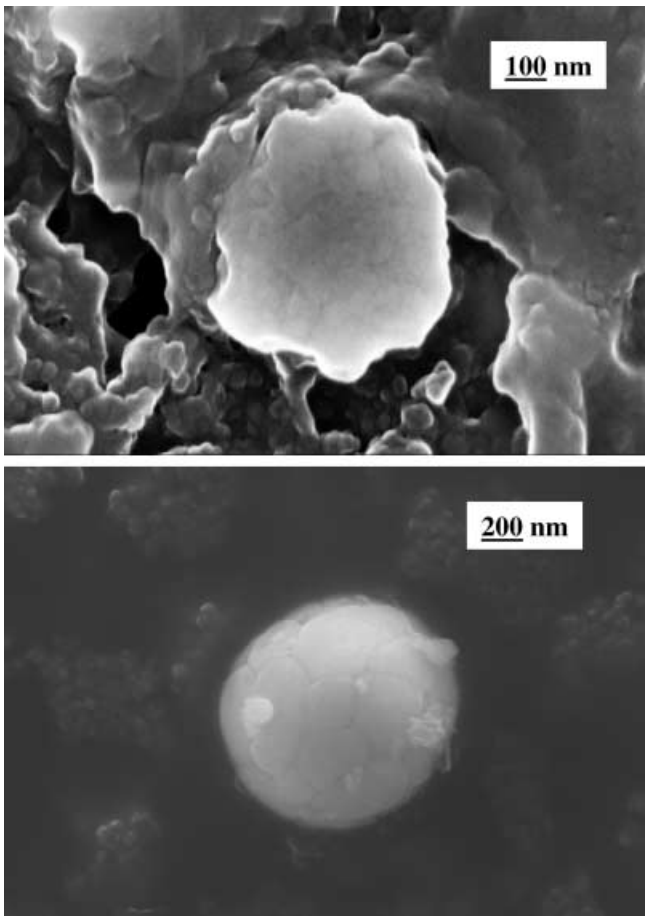

Figure 6. a and 6b. MgF_2 combustion particles.

Since T_{eq} for reaction (12) – which should be the main reaction of Mg in the vapour phase – is much higher than the vaporization/dissociation temperature for MgF_2, it can be assumed that the dispersed Mg particles are fully consumed by the fluorination process which is in contrast to Mg/O_2 or $Mg/NaNO_3$ combustion where condensed MgO precipitates on liquid Mg-particles[26]. REM photographs of MT combustion residue indeed show MgF_2 particles having diameters of about 30 nm to 50 nm thus indicative of condensation of gaseous MgF_2[24]. Figure 6a shows a polished section microphotograph of the inner core of a MgF_2-particle of which the constitution was determined by X-ray fluorescence. It can be seen that coalescence of small MgF_2-particles/droplets having a diameter of about 30 nm to 50 nm yield agglomerates of up to several μm in diameter becoming spherical again as can be seen from Figure 6b.

3.1 Burning Rate

Although T_f is a function of ξ(Mg) the burning rate r ($mm \cdot s^{-1}$) does not correlate with it as is the case with many AP composite propellants[27]. The burning rate of MTV r is dependent on the ξ(Mg), the ambient pressure p and the grain sizes ϕ_{Mg}, ϕ_{PTFE} (μm), which are more practically described with the specific surface a_{Mg} and a_{PTFE} ($m^2 \cdot g^{-1}$).

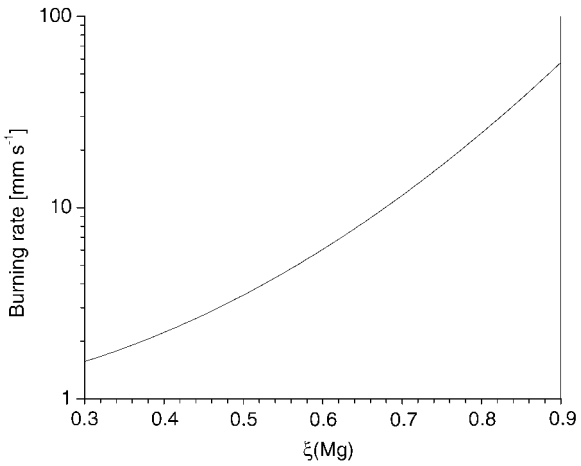

Figure 7. Typical $r = f(\xi(Mg))$ plot.

3.1.1 Stoichiometric Effects

The burning rate of MTV, in general, shows exponential dependence on the weight fraction of ξ(Mg). The influence of stoichiometry on the burning rate has been investigated by Cudzilo[15], Koch[28], Kubota[29,30], Kuwahara[31] and Peretz[32]. Figure 7 shows the typical shape of a $r = f(\xi(Mg))$ plot.

Although individual experimental series applying defined granular sizes ϕ_{Mg}, ϕ_{PTFE}, and defined ambient pressure are designed in a similar way the r values for the maxima might vary as strongly as by a factor of four. Likewise, the maximum might shift from $\xi(Mg) = 0.65 - 0.8$ by changing from small to larger particle sizes. With rising ξ(Mg) numerous Mg-particles are ejected to the gas phase and the flame size is enlarged[24]. This is in contrast to the observation with $Mg/NaNO_3$ pyrolants that show particle ejection only at stoichiometric ratios and show small flames at fuel rich conditions[33].

3.1.2 Pressure Dependence

The combustion of pyrotechnics is often dependent on the ambient pressure as can be described according to Vielle's law, Eq. (18):

$$r = a \cdot P^n \tag{18}$$

with:

$a =$ coefficient describing the influence of temperature on rate of combustion

$n =$ pressure exponent describing the influence of pressure on rate of combustion.

The pressure dependence of the MTV burning rate was investigated by Kuwahara[31], Kubota[29,30] and Peretz[32]. According to their results fuel rich compositions $\xi(Mg) > 0.7$ display a low pressure exponent $n \sim 0.06$ thus indicating that the propagation of the reaction in fuel rich compositions is mainly dependent on the thermal conductivity of the solid

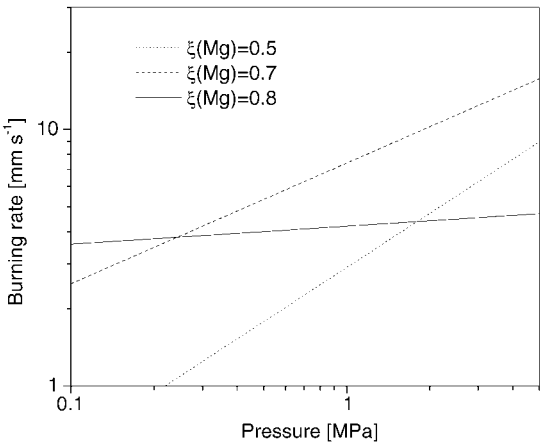

Figure 8. $r = f(p)$ plots for three MT pyrolants.

composition. In addition, the burning rate law is cubic in shape. With lower magnesium weight fraction $\xi(Mg) < 0.6$ the pressure exponent reaches values beyond 0.7 and exhibits linear behaviour. Figure 8 displays $r = f(p)$ plots of several MTV pyrolants with values given by Kuwahara[31].

3.1.3 Influence of the Grain Size on the Burning Rate

The influence of both Mg and PTFE grain sizes and ratio of grain sizes on the burning rate at atmospheric pressure and higher pressures was determined by Kubota[29,30] and Kuwahara[31].

At atmospheric pressure and at lower pressure mixtures having $omega = \frac{\phi(Mg)}{\phi(PTFE)} < 0.05$ display the highest possible burning rate at a given stoichiometry. In addition, fuel rich compositions with $\omega < 0.05$ show only a low pressure exponent n thus being only slightly influenced by ambient pressure. Likewise high ω-values (>10) lead to very low burning rates and exhibit also high burning rate exponents.

In Ref. 31 a mathematical model for the influence of grain size on the burning rate is given which will be discussed later on c.f. Section 3.1.6.

Scheme 3 shows the functional relationship of several parameters on the burning rate.

3.1.4 Mathematical Model for the Burning Rate of MT Pyrolants

The burning rate of a pyrolant system is determined by two factors. The first is the heat of reaction evolved in either condensed and gas phase as well as the energetic balance at the burning surface, which is determined by either vaporization of metallic fuel and decomposition of an oxidizer. The second factor is the heat transfer between gas phase, burning surface, preignition zone and pyrolant at ambient temperature influencing the burning rate.

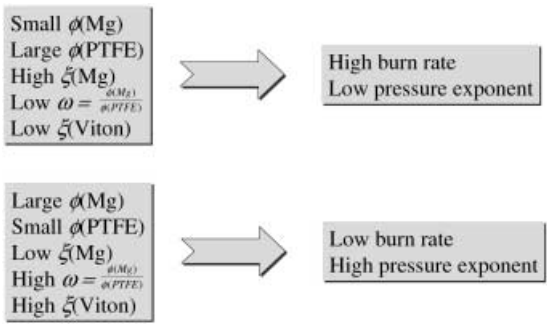

Scheme 3. Burning rate functional relationship.

Kubota[29] has been the first to thoroughly investigate the burning rate of Mg/PTFE pyrolants and to propose a mathematical model, which takes into account experimentally measured values. We will consider this model later.

In view of the experimental findings (c.f. Section *2.3.2.1)* the combustion of MTV may be separated in three stages being:

a) Pre-ignition reaction, that is Grignard type species formation and subsequent MgF_2 + olefin release
b) Surface reaction, that is fusion and/or vaporization of Mg and depolymerization of molten PTFE, and
c) Gas phase combustion of Mg with C_xF_y, F_2 species.

Addressing stage a) one encounters a relatively simple problem which may be assumed an exothermic condensed phase reaction.

The burning rate of this type of reaction can be easily described applying McLain's model of delay type compositions, Eq. (19)[34]:

$$r = \frac{\lambda \cdot Q}{c_p^2 \cdot \rho \cdot b \cdot (T_s - T_0)} \tag{19}$$

The parameters are as follows:

λ = thermal conductivity of composition [$J \cdot s^{-1} \cdot m^{-1} \cdot K^{-1}$]
Q = heat of reaction of pre-ignition reaction, that is Grignard formation + reductive elimination [$J \cdot kg^{-1}$]
b = unit size of strand width [m]
c_p = specific heat of composition [$J \cdot kg^{-1} \cdot K^{-1}$]
ϱ = density of composition [$kg \cdot m^{-3}$]
T_s = temperature of reaction zone [K]
T_0 = ambient temperature [K]

The thermodynamic properties of the binary composition are considered to be sums of the properties of both constituents Mg and PTFE. The respective values are given in Table 1. The reaction enthalpy for the preignition reaction, Eq. (7), can be calculated from the single reaction steps.

$$Mg + (-C_2F_4-)_n \rightarrow (-CF_2-CFMgF-)_n + 170\ kJ \cdot mol^{-1} \tag{20}$$

$$(-CF_2-CFMgF-)_n \rightarrow (-C_2F_2-)_n + MgF_2 + 1124\ kJ \cdot mol^{-1} \tag{21}$$

Table 2. Propagation rate of the preignition reaction as a function of ξ(Mg), λ and Q.

ξ(Mg)	Q [J kg^{-1}]	λ[J s^{-1} m^{-1} K^{-1}]	r [mm s^{-1}]
0.30	1.94E + 09	46.9708	1.80966
0.35	2.27E + 09	54.7586	2.56211
0.40	2.59E + 09	62.5464	3.48342
0.45	2.91E + 09	70.3342	4.59230
0.50	3.24E + 09	78.1220	5.90953
0.55	3.56E + 09	85.9098	7.45813
0.60	3.89E + 09	93.6976	9.26367
0.65	4.21E + 09	101.4854	11.35458
0.70	4.53E + 09	109.2732	13.76246
0.75	4.86E + 09	117.0610	16.52251
0.80	5.18E + 09	124.8488	19.67398
0.85	4.48E + 09	132.6366	18.93942
0.90	2.99E + 09	140.4244	14.01172

Since MTV displays gas phase combustion it has to be assumed that only a certain fraction of both Mg and PTFE react with each other in the PIR. From the DSC investigation (c.f. Section 2.3.2.1) of stoichiometric MT mixture (ξ(Mg) = 0.3) it is evident that 440 J · g^{-1} are released in the condensed phase in the range up to 600 °C. If we assume the maximum possible heat of reaction in the condensed phase to equal the heat of reaction in Eq. (2) of Ref. 1 (−1439 kJ · mol^{-1}) then it follows that about 7.4% of the magnesium present in the compositions react with PTFE as was confirmed by Kuwahara[35], thus the heat of reaction is the weight fraction of magnesium ξ(Mg) × 0.074 x the sum of the reaction enthalpies of the above reaction steps (Table 2). Given the temperature of the PIR zone to be ∼500 K, as was determined by Kubota, then the propagation rate for the PIR follows a cubic law (Figure 9) showing the maximum burning rate at ξ(Mg) = 0.8 and declining again at higher ξ(Mg) values, which has been observed likewise in praxi.

Addressing stage b) and c) we assume steady state combustion. Hence, the burning rate r that is recession of the burning surface is mainly dependent on heat transfer $\dot{q}_s$ from the gas phase[36] and can thus be calculated applying

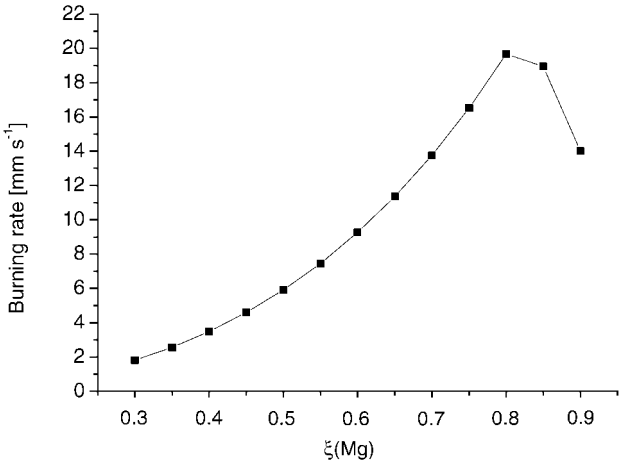

Figure 9. Propagation rate of the preignition reaction in the condensed phase.

Eq. (22). It is further assumed that the heat of vaporization of PTFE is the negative value of the heat of polymerisation of PTFE. In addition, it is assumed that magnesium is dispersed as liquid droplets.

$$r = \frac{\dot{q}_s}{\rho \cdot H_v} \tag{22}$$

with:

$\dot{q}_s$ = heat flux to the burning surface [J · s^{-1} · m^{-2}]
ρ = density of the composition [kg · m^{-3}]
H_v = enthalpy of vaporization of PTFE and melting of Mg [J · kg^{-1}]

The heat flux is the sum of both conductive heat transfer and radiative heat transfer:

$$\dot{q}_s = \dot{q}_t + \dot{q}_r \tag{23}$$

To calculate the contribution of conductive heat transfer we apply the Fourier equation:

$$\dot{q}_t = \lambda \cdot \frac{T_f - T_s}{\delta} \tag{24}$$

with:

$\dot{q}_t$ = heat flux via transfer [J · s^{-1} · m^{-2}]
λ = thermal conductivity of transfer medium [J · s^{-1} · m^{-1} · K^{-1}]
T_f = flame temperature [K]
T_s = burning surface temperature [K]
δ = thickness of the transfer medium [m]

The thickness of the transfer medium which is the gas phase has been determined by Kubota to be ∼10^{-6} m[29]. The flame temperature for burning MT and thermal conductivity of the gas phase can be determined applying common numerical codes as the NASA-CEA code. The burning surface temperature has been determined by Kubota to equal values of about 1000 K[29].

The heat flux via heat transfer was calculated for 13 compositions, ξ(Mg) = 0.30–0.90 (Table 3) and is shown in Figure 10.

In addition, the radiative heat transfer from the gas phase to the burning surface has to be considered. Therefore, we apply the following Eq. (25):

$$\dot{q}_r = r_{ex} \cdot \left(T_f^4 - T_s^4\right) \tag{25}$$

$$r_{ex} = \frac{\sigma}{\left(\frac{1}{\varepsilon_f} + \frac{1}{\varepsilon_s} - 1\right)} \tag{26}$$

with:

$\dot{q}_r$ = radiative heat transfer [J · s^{-1} · m^{-2}]
r_{ex} = radiation exchange number
σ = Stephan Boltzmann constant [5.67051 · 10^{-8} J · s^{-1} · m^{-2} · K^{-4}]
ε_f = emissivity of the gas phase [1]
ε_s = emissivity of the surface

The emissivity of the gas phase is assumed to be ∼0.5[28]. Because of the presence of melted liquid magnesium, the

Table 3. Conductive heat transfer as function of ξ(Mg), T_f, T_s and λ.

ξ(Mg)	T_f [K]	T_s [K]	λ [J s^{-1} m^{-1} K^{-1}]	q′ [W m^{-2}]
0.30	3147	1149	0.1407	11244744
0.35	3361	1131	0.1426	12723488
0.40	3089	1114	0.1303	10292120
0.45	2503	1097	0.1105	6216770
0.50	2358	1079	0.1059	5419890
0.55	2269	1062	0.1045	5043812
0.60	2128	1044	0.1013	4393235
0.65	1787	1027	0.0887	2696784
0.70	1364	1009	0.0703	997976
0.75	1364	992	0.0703	1045766
0.80	1364	975	0.0703	1093557
0.85	1364	957	0.0703	1144158
0.90	1364	940	0.0703	1191949

Table 4. Radiative heat transfer as function of ξ(Mg), T_f and T_s.

ξ(Mg)	T_f [K]	T_s [K]	q′ [W m^{-2}]
0.30	3147	1149	496626
0.35	3361	1131	649380
0.40	3089	1114	461416
0.45	2503	1097	194870
0.50	2358	1079	152382
0.55	2269	1062	130079
0.60	2128	1044	99586
0.65	1787	1027	46834
0.70	1364	1009	12501
0.75	1364	992	12852
0.80	1364	975	13185
0.85	1364	957	13520
0.90	1364	940	13819

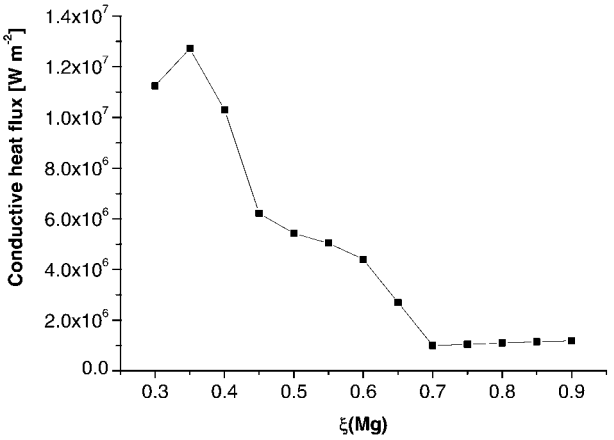

Figure 10. Heat flux via heat transfer from the gas phase to the burning surface.

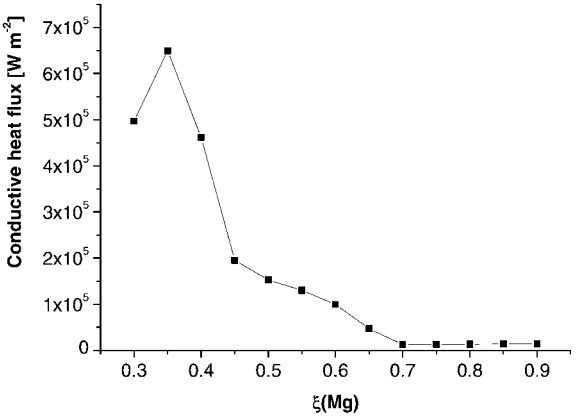

Figure 11. Heat flux via radiative heat transfer from the gas phase to the burning surface.

emissivity of the burning surface can be assumed to be similar to polished magnesium which is ∼0.1.

The heat flux via radiative heat transfer was calculated for 13 compositions, ξ(Mg) = 0.30–0.65 (Table 4) and is shown in Figure 11.

The values obtained for both – conductive and radiative heat transfer – are added and applied to Eq. (22). The enthalpy of vaporization of both Mg and PTFE were calculated on the basis of stoichiometry and considered additive.

$$H_v = \xi \cdot (H_v(Mg)) + ((1-\xi) \cdot H_v(PTFE)) \quad (27)$$

$$H_v(PTFE) = \int_{T_0}^{T_s} c_p dT + H_{dep} \quad (28)$$

$$H_v(Mg) = \int_{T_0}^{T_s} c_p dT + H_{melt} \quad (29)$$

$$H_v(PTFE) = 1020 \cdot (555-298) + 1.72 \cdot 10^6 = 1\,926\,000\ \mathrm{J \cdot kg^{-1}}$$

$$H_v(Mg) = 1023 \cdot (500-298) + 371\,900 = 578\,600\ \mathrm{J \cdot kg^{-1}}$$

The burning rate was calculated for 13 stoichiometries between ξ(Mg) = 0.3–0.90 (Table 5) and is shown in Figure 12.

The functional burn rate behaviour displayed in Figure 12 is quite unrealistic. Experience teaches us, that burn rates rise from stoichiometric oxidiser/fuel ratio with increasing magnesium weight fraction ξ(Mg) to reach a maximum at ξ(Mg) ∼0.8 and to decline again at higher values.

Nevertheless if we add burn rate values from both preignition reaction and contribution from gas phase heat transfer we obtain a curve showing good agreement with actual experimental data, as is shown in Figure 13.

This would imply that the burn rate is mainly affected by the thermochemistry of the condensed phase and that heat transfer mechanisms from the gas phase to the burning surface do not play a major role in controlling the burn rate with MTV compositions. In view of the unaffected burn rate at fuel rich stoichiometries by ambient pressure such an interpretation seems quite likely. Nevertheless with real pyrolant systems which always display an unavoidable porosity burn rate enhancement due to filtration of vaporised species into the condensed phase especially at higher ambient pressures must be considered in low ξ(Mg) range.

Table 5. Burn rate as function of ξ(Mg), T_f and λ.

ξ(Mg)	H_v [J kg^{-1}]	T_f [K]	q′ [W m^{-2}]	r [mm s^{-1}]
0.30	$1.56098 \cdot 10^6$	3147	11741370	3.5175
0.35	$1.49081 \cdot 10^6$	3361	13372868	4.2517
0.40	$1.42063 \cdot 10^6$	3089	10753536	3.6371
0.45	$1.35046 \cdot 10^6$	2503	6411640	2.3130
0.50	$1.28029 \cdot 10^6$	2358	5572272	2.1504
0.55	$1.21012 \cdot 10^6$	2269	5173891	2.1427
0.60	$1.13995 \cdot 10^6$	2128	4492821	2.0039
0.65	$1.06978 \cdot 10^6$	1787	2743618	1.3232
0.70	$9.99610 \cdot 10^5$	1364	1010477	0.5294
0.75	$9.29440 \cdot 10^5$	1364	1058618	0.6055
0.80	$8.59269 \cdot 10^5$	1364	1106742	0.6953
0.85	$7.89098 \cdot 10^5$	1364	1157678	0.8044
0.90	$7.18927 \cdot 10^5$	1364	1205768	0.9343

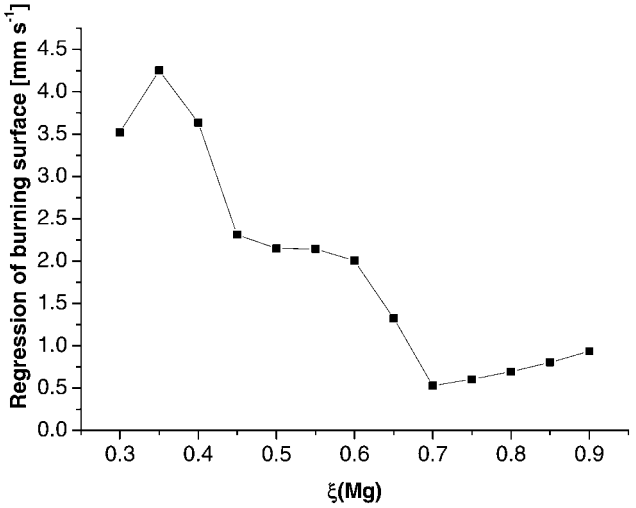

Figure 12. Burning rate as function of the combined heat flux from the gas phase to the burning surface.

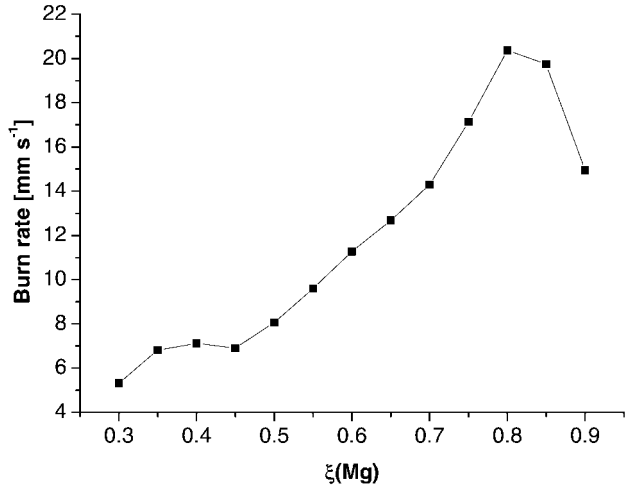

Figure 13. Burn rate as a function of both heat flux from gas phase and preignition reaction

3.1.5 *Combustion Rate Measurement of the 70/30 Mg/PTFE Pyrolant in Air and in Argon*

To prove the prediction, that gas phase reactions do not influence the burning rate, strands of Mg/PTFE (70/30) pyrolant were burnt under ambient air and argon. In the first case, the burning rates should be influenced by both condensed phase and gas phase combustion. In the latter case only primary gas phase combustion and condensed phase combustion should affect the burning rate. Afterburning of Mg and C should be impossible in case of an argon atmosphere.

The measurements were made with strands consolidated with 120 MPa. The strands were ignited with a piece of quick match and burnt on the bottom of a steel vessel of 50 cm height and 20 cm diameter purged with air or argon of 0.1 MPa pressure. The applied argon was of 5.0 purity. The burning rate for the cylindrical samples was measured with a video camera timer.

The mean burning rate in air for five measurements was 5.2 ± 0.3 mm $\cdot$ s^{-1}.

The mean burning rate in argon for five measurements was 5.1 ± 0.3 mm $\cdot$ s^{-1}.

Changing from argon to air after completion of the reaction leads to a glowing of the dispersed residues thus indicating the presence of unreacted somewhat "pyrophoric" magnesium.

Although the burning rate under argon atmosphere is a little slower than in air the result indicates that the burning rate at high ξ(Mg) values is mainly affected by the thermal conductivity of the condensed phase. This is in contrast to the combustion model developed by Kubota[29], who assumed that the heat flux from the gas phase combustion zone $\dot{q}_s$ mainly determines the burning rate r as is the case with conventional AP composite propellants.

About thirty years ago, Dillehay made the same observation with $Mg/NaNO_3$ flares[37]. Although he observed the candlepower to decrease dramatically to about 1.5% of its original value by changing from air to argon at ξ(Mg) = 0.6, the burning rate was unaffected by the atmosphere and remained the same under argon. Similarly as with MT pyrolants, the rate determining process with $Mg/NaNO_3$ pyrolants is assumed to occur in the condensed phase[38]. Likewise, Griffiths et al.[25] reported equal burning rates for unspecified MT pyrolants in either air and argon atmosphere.

3.1.6 *Comparison of Combustion Models*

As mentioned above a series of models for MTV combustion has been proposed. Kubota in his analytical model[29] assumed the heat flux $\dot{q}_s$ to be determined by:

$$\dot{q}_s = \rho_p \cdot c_p \cdot r \cdot \left(T_s - T_0 - \frac{H_v}{c_p} \right) \tag{30}$$

which may be simplified by inserting $\Delta T = T_s - T_0$ to give:

$$r = \frac{\dot{q}_s}{\rho_p \cdot (\Delta T \cdot c_p - H_v)} \tag{31}$$

which is identical to Eq. (22). Although Eq. (31) is valid to take into account the influence of the gas phase on the rate of recession of the burning surface as discussed above, Kubota did not take into account the deviation of T_f and r for heterogeneous pyrolants in contrast to homogeneous propellants. From Eqs. (24, 25 and 26) we see that with decreasing T_f, $\dot{q}_s$ can not increase and thus $\dot{q}_s$ can not be responsible for the observed burning rate behaviour (c.f. section 3.1.1).

Kuwahara in his analytical model on the combustion process of *MTV* (Eq. 32) takes into account the particle size of Mg to explain the different burning rates observed[35] with either small and large Mg particles assumed to be spherical.

$$r = \frac{1}{\delta_{MgF_2}} \cdot \sqrt[3]{\frac{1}{\rho_{MT} \cdot \xi(Mg)}} \cdot \sqrt[3]{\frac{\pi}{6 \cdot \rho_{Mg}}} \cdot r_{Mg} \cdot \phi_{Mg} \tag{32}$$

with:

δ_{MgF2} = thickness of the MgF_2 layer on a Mg particle of diameter ϕ_{Mg} after DSC experiment [μm]
ρ_M = density of the pyrolant [$g \cdot cm^{-3}$]
r_{Mg} = Mg particle burning rate in a PTFE pyrolant environment [$mm \cdot s^{-1}$]

Although this model does not consider thermal effects such as conductivity or heat of reaction, both the Mg particle burning rate r_{Mg} and the thickness of the MgF_2 layer are linked to the heat of reaction and the thermal conductivity of the pyrolant.

In contrast to Kubota's model, no assumptions concerning the combustion mechanism are made.

4 Conclusion

It could be shown, that Magnesium/Teflon®-pyrolants form some type of fluoro-Grignard species as reactive intermediate in the condensed phase upon combustion in the preignition reaction. These decompose at higher temperature in a reductive elimination reaction to yield magnesium fluoride and a partially olefinic polymer. At the surface of the pyrolant magnesium is dispersed as either vapour or liquid droplets in the gas phase. Likewise, the fluoropolymer is depolymerized to give mainly the monomer tetrafluoroethylene which dissociates to give difluorocarbene and tetrafluoromethane. These fluorocarbons react with the dispersed magnesium to give magnesium fluoride and soot. At present there is some indication that the burning rate of Magnesium/Teflon® pyrolants is mainly influenced by the thermal conductivity of the condensed phase and the exothermicity of the preignition reaction which is the fluoro-Grignard formation and the release of magnesium fluoride and the partially olefinic polymer.

Further research is in progress to reveal the influence of both the preignition reaction as well as the gas phase combustion on the burning rate.

Radiation behaviour, processing, ageing and safety features of MTV will be addressed in an future article.

5 References

(1) E.-C. Koch, "Development and Application of Magnesium/Teflon/Viton (MTV)", *Propellants, Explosives, Pyrotechnics* 27, 262 – 266 (2002).
(2) B. J. McBride and S. Gordon, "Computer Program for Calculation of Complex Chemical Equilibrium Compositions and Applications", *NASA RP 1131*, June 2000.
(3) R. L. Tischer, "Effect of Entrained Air in Determining Optimum Flare Compositions", *2nd Int. Pyrotechnics Seminar*, Aspen, CO, USA, July 20 – 24, 1970, pp. 423 – 445.
(4) L. V. De Yong, K. J. Smit, *"A Theoretical Study of the Combustion of MTV Pyrotechnic Composition"*, MRL-TR-91-25, DSTO Materials Research Laboratory, Melbourne, (1991).
(5) F. C. Christo, *"Thermochemistry and Kinetics Models for Magnesium/Teflon/Viton Pyrotechnic Compositions"*, *DSTO-TR-0938*, DSTO Aeronautical and Maritime Research Laboratory, Melbourne, (1999).
(6) G. Krien, "*Thermoanalytische Ergebnisse von pyrotechnischen Ausgangsstoffen",* Az.: 3.0-3/3712/75, BICT, Swisttal-Heimerzheim (1975).
(7) J. Falbe, M. Regitz (eds.), "*Römpp Chemielexikon"*, 9th ed., Georg Thieme Verlag, Stuttgart, New York 1995, Vol. 5, p. 3573.
(8) B. B. Baker, D. J. Kasparyk, "Thermal Degradation of Commercial Fluoropolymers in Air", *Polymer Degradation and Stability 42,* 181 – 188 (1993).
(9) T. T. Griffiths, J. Robertson, P. G. Hall, and R. T. Williams, "Thermal Decomposition of PTFE in the Presence of Magnesium", *16th Int. Annual Conference of ICT* , Karlsruhe, July 2 – 5, 1985, pp. 19/1 – 10.
(10) G. Speckhofer, R. Gilles, W. Smith, and M. Bures, "A Consistent Set of Thermodynamic Properties and Transport Coefficients for High Temperature Plasmas", *14th Int. Symp. Plasma Chemistry*, Inst. Plasma Physics, Acad. Sci. Czech Rep., Prague, (1999).
(11) N. Watanabe, T. Nakajima, and H. Touhara, "*Graphite Fluorides"*, Elsevier Publishers, Amsterdam 1988, p. 122.
(12) E.-C. Koch, "Fluoreliminierung aus Graphitfluorid mit Magnesium", *Z. Naturforsch. 56b,* 512 – 516 (2001).
(13) V. M. Chumarev, V. P. Mar'evich, and A. A. Shtin, "Thermal Decomposition of Polytetrafluoroethylene", *Russian Journal of Applied Chemistry 71,* 1861 – 1862 (1998).
(14) G. Krien, *"Thermoanalytische Ergebnisse der Untersuchung von pyrotechnischen Sätzen",* Az.: 3.0 – 3/5446/81, BICT, Swisttal-Heimerzheim (1981).
(15) S. Cudzilo, W. Trzcinski, "Badanie procesu spalania mieszanin metal-politetrafluoroetylen", *Biuletyn Wat*, *45* 131 – 149 (1996).
(16) S. Cudzilo, W. A. Trzcinski, "Calorimetric Studies of Metal/Polytetrafluoroethylene Pyrolants", *Pol. J. Appl. Chem. 45,* 25 – 23 (2001).
(17) X. Wang, H. R. Harris, K. Bouldin, H. Temkin, S. Gangopadhyay, M. D. Strahtman, and M. West, *"Structural Properties of Fluorinated Amorphous Carbon Films",* www.phys.ttu.edu/ ~ gango/paper2.html.
(18) J. Weidlein, U. Müller, and K. Dehnicke, „*Schwingungs-Hauptgruppenelemente*", Georg Thieme Verlag, Stuttgart, New York 1981, p. 240.

(19) P. G. Jasien, C. E. Dykstra, "Simplest Magnesium Cluster Grignard. Theoretical Evidence for Strong Metal-Metal Stabilization of RMg_2X Species", *J. Am. Chem. Soc. 105,* 2089 – 2090 (1983).
(20) P. G. Jasien, C. E. Dykstra, "The Influence of a Second Magnesium Atom in Unsolvated Magnesium-Hydrogen Halide Reaction", *J. Am. Chem. Soc. 107,* 1891 – 1895 (1985).
(21) L. Liu, S. R. Davis, "Ab Initio Study of the Grignard Reaction Between Magnesium Atoms and Fluoroethylene and Chloroethylene", *J. Phys. Chem. 95,* 8619 – 8625 (1991).
(22) S. R. Davis, "Ab Initio Study of the Insertion Reaction of Mg into the Carbon-Halogen Bond of Fluoro- and Chloromethane", *J. Am. Chem. Soc. 113,* 4145 – 4150 (1991).
(23) I. Glassman, "Combustion of Metals" in: M. Summerfield (ed.) "*Progress in Astronautics and Aeronautics*", *Vol 1* "*Solid Propellant Research"*, Academic Press, New York and London 1960, pp. 253 – 258.
(24) E.-C. Koch, unpublished work (2000).
(25) V. S. Griffiths, D. C. A. Izod, E. O. Sullivan, "Some Observations of some Pyrotechnic Compositions", *2nd Int. Pyrotechnics Seminar*, Aspen, CO, USA, July 20 – 24, 1970, pp. 449 – 471.
(26) E. L. Dreizin, "Phase changes in metal combustion", *Progress in Energy and combustion Science 26,* 57 – 78 (2000).
(27) T. Kuwahara, N. Kubota, "Role of Boron in Burning Rate Augmentation of AP Composite Propellants", *Propellants, Explosives, Pyrotechnics 14,* 43 – 46 (1989).
(28) E.-C. Koch, A. Dochnahl, "IR Emission Behaviour of Magnesium/Teflon/Viton (MTV) Compositions, *Propellants, Explosives, Pyrotechnics 25,* 37 – 40 (2000).
(29) N. Kubota, C. Serizawa, "Combustion Process of Mg/TF Pyrotechnics", *Propellants, Explosives, Pyrotechnics 12,* 145 – 148 (1987).
(30) N. Kubota, C. Serizawa, "Combustion of Magnesium/Polytetrafluoroethylene", *J. Propulsion 3,* 303 – 307 (1987).
(31) T. Kuwahara, S. Matsuo, and N. Shinozaki, "Combustion and Sensitivity Characteristics of Mg/Tf Pyrolants, *Propellants, Explosives, Pyrotechnics 22,* 198 – 202 (1997).
(32) A. Peretz, "Investigation of Pyrotechnic MTV Compositions for Rocket Motor Igniters", *18th Joint Propulsion Conf.*, Cleveland, Ohio, June 21 – 23, 1982, AIAA-82-1189 (1982).
(33) R. B. Rao, P. S. Rao, and H. Singh, "Prediction of Burn Rate of Magnesium-Sodium Nitrate Propellant", *Combust. Sci. and Tech. 108,* 133 – 147 (1995).
(34) J. H. McLain, *Pyrotechnics*, The Franklin Institute Press, Philadelphia 1980, p. 48.
(35) T. Kuwahara, T. Ochiachi, "Burning rate of Mg/TF-Pyrolants", *18th Int. Pyrotechnics Seminar*, Breckenridge, CO, 13 – 17 July 1992, pp. 539 – 549.
(36) I. Hadar, A. Gany, "Fuel Regression Mechanism in a Solid Fuel Ramjet", *Propellants, Explosives, Pyrotechnics 17,* 70 – 76 (1992).
(37) D. R. Dillehay, "Illuminant Performance in Inert Atmospheres", 4*th Int. Pyrotechnics Seminar*, Steamboat Village, CO, July 22 – 26, 1974, p. 2.
(38) J. R. Ward, L. J. Decker, and A. W. Barrows, "Burning Rate of Pressed Strands of a Stoichiometric Magnesium-Sodium Nitrate Mix", *Combustion and Flame 51,* 121 – 123 (1983).

(Received June 7, 2002; Ms 2002/029)